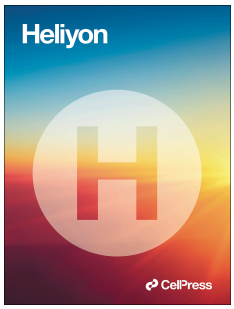

Changes within the P681 residue of spike dictate cell fusion and syncytia formation of Delta and Omicron variants of SARS-CoV-2 with no effects on neutralization or infectivity

Alona Kuzmina, Dina Korovin, Ido Cohen lass, Nofar Atari, Aner Ottolenghi, Pan Hu, Michal Mandelboim, Benyamin Rosental, Elli Rosenberg, Felipe Diaz-Griffero, Ran Taube

PII: S2405-8440(23)03957-9

DOI: https://doi.org/10.1016/j.heliyon.2023.e16750

Reference: HLY 16750

To appear in: *HELIYON*

Received Date: 27 November 2022

Revised Date: 13 April 2023

Accepted Date: 25 May 2023

Please cite this article as: , Changes within the P681 residue of spike dictate cell fusion and syncytia formation of Delta and Omicron variants of SARS-CoV-2 with no effects on neutralization or infectivity, *HELIYON* (2023), doi: https://doi.org/10.1016/j.heliyon.2023.e16750.

Changes within the P681 residue of spike dictate cell fusion and syncytia formation of Delta and Omicron variants of SARS-CoV-2 with no effects on neutralization or infectivity

Alona Kuzmina[1], Dina Korovin[1], Ido Cohen lass[1], Nofar Atari[4], Aner Ottolenghi[1,3], Pan Hu[2], Michal Mandelboim[4,6], Benyamin Rosental[1,3], Elli Rosenberg[5], Felipe Diaz-Griffero[2] and Ran Taube[1*]

[1]The Shraga Segal Department of Microbiology Immunology and Genetics Faculty of Health Sciences, Ben-Gurion University of the Negev, Israel.

[2] Department of Microbiology and Immunology, Einstein, Bronx, NY 10461

[3] Regenerative Medicine and Stem Cell Research Center, Ben Gurion University of the Negev.

[4] Central Virology Laboratory, Public Health Services, Ministry of Health and Sheba Medical Center, Tel-Hashomer, Israel.

[5] Soroka Medical Center, Beer Sheva, Israel.

[6] Department of Epidemiology and Preventive Medicine, School of Public Health, Sackler Faculty of Medicine, Tel Aviv, Israel.

[*] Lead contact and correspondence author: Ran Taube, Ph.D.

email: rantaube@bgu.ac.il;

Running Title: P681 mutations with SARS-CoV-2 spike dictate fusogenicity and Syncytia formation

Keywords: SARS-CoV-2; Spike; Fusion; Syncytia; Pfizer-BTN162b2; neutralizing antibodies; Furin-Cleavage Site; Omicron-BA.1; Omicron-BA2.

Abstract

The rapid spread and dominance of the Omicron SARS-CoV-2 lineages have posed severe health challenges worldwide. While extensive research on the role of the Receptor Binding Domain (RBD) in promoting viral infectivity and vaccine sensitivity has been well documented, the functional significance of the $_{681}$PRRAR/SV$_{687}$ polybasic motif of the viral spike is less clear. In this work, we monitored the infectivity levels and neutralization potential of the wild-type human coronavirus 2019 (hCoV-19), Delta, and Omicron SARS-CoV-2 pseudoviruses against sera samples drawn four months post administration of a third dose of the BNT162b2 mRNA vaccine. Our findings show that in comparison to hCoV-19 and Delta SARS-CoV-2, Omicron lineages BA.1 and BA.2 exhibit enhanced infectivity and a sharp decline in their sensitivity to vaccine-induced neutralizing antibodies. Interestingly, P681 mutations within the viral spike do not play a role in the neutralization potential or infectivity of SARS Cov-2 pseudoviruses carrying mutations in this position. The P681 residue however, dictates the ability of the spike protein to promote fusion and syncytia formation between infected cells. While spike from hCoV-19 (P681) and Omicron (H681) promote only modest cell fusion and formation of syncytia between cells that express the spike-protein, Delta spike (R681) displays enhanced fusogenic activity and promotes syncytia formation. Additional analysis shows that a single P681R mutation within the hCoV-19 spike, or H681R within the Omicron spike, restores fusion potential to similar levels observed for the Delta R681 spike. Conversely, R681P point mutation within the spike of Delta pseudovirus abolishes efficient fusion and syncytia formation. Our investigation also demonstrates that spike proteins from hCoV-19 and Delta SARS-CoV-2 are efficiently incorporated into viral particles relative to the spike of Omicron lineages. We conclude that the third dose of the Pfizer-BNT162b2 provides appreciable protection against the newly emerged Omicron sub-lineages. However, the neutralization sensitivity of these new variants is diminished relative to that of the hCoV-19 or Delta SARS-CoV-2. We further show that the P681 residue within spike dictates cell fusion and syncytia formation with no effects on the infectivity of the specific viral variant and on its sensitivity to vaccine-mediated neutralization.

Introduction

In December 2019, a new virus of the Severe Acute Respiratory Syndrome Coronavirus (SARS-CoV)-related coronavirus species was identified in China in and classified as the pathogenic cause of COVID-19. Over 600 million cases were diagnosed, and as of February 2023, above 7.5 million death tolls were reported globally [1, 2]. In an attempt to limit viral spread, several authorized vaccines were developed, among them the BNT162b2-Pfizer mRNA vaccine and the 1273 Moderna mRNA vaccines were primarily administrated. For both of these vaccines, two doses were administered to produce anti-spike antibodies that can target the SARS- CoV-2 full-length spike protein of the hCoV-19 spike protein, thus providing efficient protection against viral infection and disease progression [3-8] [9-12] [13, 14]. However, the rapid and efficient viral spread enhanced the accumulation of variants that exhibit spike mutations, primarily at the receptor binding domain domain that mediates binding to the human ACE2 receptor. These mutations often result in an improved affinity of spike to ACE2, and serves as a mechanism to evade the immune response and neutralizing antibodies. Overall, emerged viral variants exhibited reduced sensitivity to the vaccines, thus leading to an evaluation regarding the administration of supplementary boosts.

Early viral strains that have been defined as Variants Of Concern (VOC) include Alpha [15] and Beta [16, 17] [18-28], which were quickly dominated by Delta variant that causes severe clinical symptoms [29-31]. To battle against the waning of vaccine-elicited antibody immune response to emerging VOCs, a third dose of vaccine was approved in mid-2021, first in Israel and later worldwide. This boost has been proven to be highly effective, as it induced efficient protection and prevented disease progression or patient hospitalization [32]. Another VOC, referred to as Omicron (B.1.1.529) emerged in late 2021, initially in South Africa, and then quickly became globally dominant. Since then, other variants, including BA.1.1., BA.2, BA.4, and BA.5, have emerged from the Omicron parental lineage strain - B.1.1.529. When compared to the original hCoV-19, Omicron sub-lineages carry several unique mutations within their spike [33, 34]. Omicron-BA.1 harbors 59 mutations within its genome, 36 of them within the spike and 15 specifically in RBD. However, there are few

mutations within spike that allows researchers to differentiate between them [33, 35, 36]. Omicron newly emerged variants partially escape vaccine-mediated protection. Moreover, in contrast to Alpha, Beta, and Delta, infection by Omicron lineages results in less severe clinical disease symptoms and lower hospitalization incidents [37-49]. To further enhance the protection of vaccine-elicited protection against the newly emerged Omicron-sub-lineages, a fourth boost of the Pfizer vaccine was initiated in Israel, providing minimal protection against emerged viruses variants with low boost efficacy of vaccine-mediated protection against viral infection [50-52]. Other countries followed this initiative, and the fourth boost is available almost everywhere.

While mutations within the spike RBD are widely investigated for their role in dictating viral infectivity and neutralization potential, the importance of the $_{681}$PRRAR/SV$_{687}$ mutations of spike, and specifically the P681 residue, is less clear. This polybasic Furin Cleavage Site (FCS) motif is unique to SARS-CoV-2 and is known to mediate entry of the viral particles via process that is dependent on TMPRSS2. While both cathepsins B and L that are both expressed in endosomes, TMPRSS2 is expressed on the surface of cells and promotes cleavage and activation of S2′ that promotes fusion between the cell and virus membranes [53, 54]. The polybasic motif of spike also promotes fusion and syncytia formation between infected cells and further facilitates TMPRSS2 endocytic viral entry that mediates the evasion of IFITM2 cellular innate response [55-60], [61]. Finally, Omicron and its sub-lineages have also exhibited lower replication levels in lung and gut cells, and their spike is not efficiently cleaved as the spike of Delta. These differences are linked with higher levels of TMPRSS2 expression [62]. Overall, the Omicron spike inefficiently utilizes TMPRSS2, with a higher dependency on endocytic entry. In agreement with these findings, the formation of syncytia between infected cells following infection with Omicron is diminished in comparison to infection by Delta. This inefficient cleavage of the Omicron spike and the inability to use TMPRSS2 possibly exerts its effects on the clinical outcomes of the Omicron variant [63, 64].

In this work, we monitored the neutralization potential of sera samples that were drawn from individuals that were vaccinated with a third dose of the BNT162b2 vaccine – at four months post-

the second dose administration. Vaccinated sera were tested against hCoV-19, its Delta, and pseudoviruses that carry the spike from Omicron-BA.1 and Omicron-BA.2 lineages. We show that relative to the hCoV-19 SARS-CoV-2 and its Delta variant, Omicron-BA.1 and Omicron-BA.2 exhibit a sharp decrease in neutralization sensitivity and elevated infectivity levels. Nevertheless, three vaccine doses still provides relative protection four months after its administration. In addition, we show that spike proteins of both Omicron BA.1 and BA.2 lineages are incorporated less efficiently into viral particles relative to the spike of hCoV-19 and Delta pseudoviruses. We then focused on the role of the proline residue at position 681 (P681) of the spike in mediating cell fusion and syncytia formation between cells that express spike. We further expressed spike proteins from hCoV-19 (P681), Delta-Arginine (R681), and Omicron-Histidine (H681) and monitored their abilities to mediate cell fusion and syncytia formation. Cell fusion was analyzed either by the GFP-split system that analyzes GFP expression as a measure of cell fusion [58], or by documenting cell fusion between transduced cells that stably express two different fluorescent reporter proteins. Our observations show that while the hCoV-19 and Omicron spike proteins promote only moderate fusogenic activity and syncytia formation, the Delta spike efficiently enhances fusion and syncytia formation between spike-expressing target cells. Introducing a single P681R mutation in the spike of hCoV-19-SARS-CoV-2 restores fusogenic potential and enhances syncytia formation of this spike. In parallel, the expression of Delta-spike protein carrying a single R681P mutation abolishes fusion potential and syncytia formation. Introducing an H681R mutation within the spike protein of Omicron restores cell fusion potential and enhanced syncytia formation, similar to those of Delta SARS-CoV-2. We therefore conclude that the P681 position of the spike is critical for mediating cell fusion and syncytia formation.

Material and Methods

RESOURCES

Lead Contact

Requests for reagents should be sent to Ran Taube (rantaube@bgu.ac.il).

Data and sample accessibility

Information regarding this manuscript can be obtained from the leading author. DNA plasmids and pseudoviruses are also available upon request.

Human subject cohort

The study was performed under the supervision of the ethical Helsinki committee at the Soroka Medical Center (protocol 0281-20-SOR). Sera samples were obtained from healthy individuals (n=35) vaccinated with the third dose of the BNT162b2 vaccine. Sera samples were collected four months post the administration of the third boost of the BNT162b2 vaccine.

Bacterial Strains and Cells

HEK293T cells that stably express the ACE2 human receptor (HEK293T-ACE2) or Vero E6 cells that express either GFP 10 or GFP 11 GFP proteins were maintained at 37^0C and 5% CO2. Cells were grown in complete DMEM media, containing glucose (Gibco), 10% FBS, 2mM GlutaMAX and 100U/ml ampicillin-streptomycin. HEK293T-ACE2 cells were generated by transducing cells with lentivirus that expresses the human ACE2 receptor. Pseudoviruses used for neutralization and infectivity experiments were normalized based on their p24 levels using ELISA. DH5α bacteria were transformed with DNA lentiviral packaging plasmids and the viral SARS-CoV-2 spike. For DNA propagation, one colony was picked and cultured in growth media at 37^0C for 10 hr while shaking.

Fusion assays

For cell-cell fusion measurements, Vero-E6 cells expressing either GFP1-10 or GFP11 were co-cultured in a 12-well plate at an equal number, and were then transfected with a total of 1μg of phCMV-SARS-CoV2-spike using TransIT-X2 (Mirus). At 24 h post-transfection, GFP fluorescence images were documented for analying cell fusion using Olympus IX73. The GFP area and the number of nuclei were quantified using ImageJ software. Fusion was defined as the percentage of GFP pixels.

Generating spike mutants

For inserting point mutations within the spike, the QuikChange Lightening Site-Directed Mutagenesis kit was used (Agilent Technologies). The hCoV-19 spike plasmid, pCG1-SARS-S-HA, that codes for the hCoV-19 spike was obtained from S. Pöhlmann at the University Göttingen [42]. For each of the indicated mutants, DNA oligos that carried the required mutation were designed. Omicron-BA.1 spike was synthetically synthesized by IDT.

Generation of pseudotyped lentivirus and neutralization assays

SARS-CoV-2 pseudoviruses were generated as previously described [31, 65]. Briefly, HEK293T cells were transfected with the following HIV packaging plasmids; pHDM-Hgpm2 that codes for a codon optimized HIV Gag-Pol (5 μg per plate; Addgene #164441); pHDM-Tat1b (3 μg per plate; Addgene #164442); pRC-CMV Rev1b (5 μg per plate; Addgene #164443) and the pHAGE-CMV-luciferase transgene (20 μg per plate). The indicated pCG1-SARS-S spike expression plasmid was also transfected (6 μg per plate) [42]. Transfection of DNA was done by $CaCl_2$ in a 10cm plate format. Viral particles were collected from the supernatant at 72 h post-transfection and filtered through 22μ [31, 65, 66]. Neutralization assays were performed in a 96-well format. SARS CoV-2 pseudutyped lentiviruses were incubated with the tested sera for 1 h at 37^{o}C. No sera samples were used as a control. The indicated pseudoviruses were then used to transduce HEK-ACE2 for 12 h, followed by replacement with complete fresh media. Following transduction, cells were harvested and their

luciferase readouts were monitored (Promega). Two neutralization experiments that are independent were conducted. In each experiment, the indicated sera samples were diluted (for each serum, 5-6 dilutions were made) and analyzed against the pseudovirus. For each dilution point, three independent dilutions were performed and analyzed. Neutralization assays were analyzed using an automated Tecan liquid handler. Readouts were used to calculate the NT_{50} – 50% inhibitory values. For monitoring the infectivity of the recombinant SARS-CoV-2 pseudoviruses, $1x10^5$ HEK293T-ACE2 cells were plated in a 12-well plate and, 24 hours later, were transduced with decreased serial dilutions. 48 hours post-transduction, cells were harvested, and their luciferase readouts were monitored. p24 ELISA measurements were conducted to ensure equal loads.

Analysis of spike incorporation into viral particles

For monitoring spike incorporation into pseudoviruses, we followed a protocol described by Schulte and colleagues [67]. Concentrated HIV-1 particles pseudotyped carrying the different SARS-CoV-2 spikes proteins were lysed with a lysis buffer that contains N-dodecyl-β-d-maltopyranoside and detected by western blot with anti-SARS-CoV-2 spike monoclonal antibody GTX632604 (GeneTex; clone 1A9) and anti-p24 (NIH repository) antibodies. For validation of spike expression, we also used a polyclonal antibody against the spike. Following SAD-PAGE and transfer to a nitrocellulose membrane, three washes in PBS-Tween were performed and membranes were incubated for 30 min with an anti-goat and anti-mouse conjugated to IRDye 680LT or IRDye 800CW (LI-COR). Bands were detected by scanning the blots using the LI-COR Odyssey Imaging System in the 700 nm or 800 nm channel.

Image analysis

Image analysis was conducted with the Scikit-image library [68] in Python 3.1. Images for each channel (GFP – fused cells; DAPI – nuclei stain) were loaded separately. Histograms for all images were equalized. Using the Otsu threshold algorithm on the GFP channel, the borders of the fused cells

were determined. The cell regions in each image were isolated and labeled using the scikit-image label algorithm, where each area corresponds to a fused cell. These regions were then iterated over and used to mask the corresponding region individually over the DAPI channel. For each iteration, the number of nuclei in the masked area, and therefore the fused cell, was assessed using the local maxima in the intensity of the DAPI image, with a minimum distance of 3 pixels between each peak. The pixel area of each region was also measured, giving us, in addition to the nuclei number in each cell, the area also. For statistical analysis, only regions with 2 or more nuclei were selected. Statistical analysis was done using a two-sided independent t-test from the stat module of the scipy [69] library. Graphing was done using the matplotlib and seaborn libraries [70]. Additional libraries were used – pandas and NumPy [71].

Statistical analysis

Statistical analyses were conducted with GraphPad Prism. The statistical significance of our study was determined by a two-tailed Student's t-test - $P \leq 0.001$. Error bars show standard deviation.

Results

Neutralizing and infectivity levels of the SARS CoV-2 Omicron pseudoviruses

Sera samples were obtained from a broad cohort of individuals that were vaccinated with three doses of the Pfizer mRNA vaccine. Samples were collected at four months post-administration of the third dose (n=35). The cohort was tested for neutralizing potency against the original hCoV-19 SARS-CoV-2, its Delta variant, and the Omicron-BA.1 and Omicron-BA.2 sub-lineages. Our neutralization assays show that in comparison to the hCoV-19 pseudovirus, Omicron-BA.2 exhibited a 12-fold decrease in neutralization potential, while Omicron-BA.1 exhibited a relative 9-fold reduction in its neutralization sensitivity to the tested sera (**Figure 1A**). Delta pseudovirus displayed only a 2-fold reduction relative to the hCoV-19 (**Figure 1A**). Despite this decrease, Omicron variants were still neutralized by the tested sera.

We then examined the infectivity of the Delta and Omicron-BA.1 and Omicron-BA.2 variants in HEK293T-ACE2 cells, comparing them to the infectivity of the hCoV-19 pseudovirus. Our findings show that Omicron-BA.1 and Omicron-BA.2 pseudoviruses exhibited 5-fold higher infectivity when compared to the hCoV-19 SARS-CoV-2. Moreover, we confirmed previous data reporting that the infectivity of the Delta variant is 2-3 fold higher compared to hCoV-19 (**Figure 1B**) [31]. Finally, as TMPRSS2 plays a role in mediating viral entry and infectivity, we over-expressed HA-TMPRSS2 in HEK293T-ACE2 cells and monitored the infectivity of SARS-CoV-2 hCoV-19 and its P681 mutants. Our data show that expression of TMPRSS2 has no role in mediating pseudovirus infectivity (**Supplementary Figure S1**). Since our analysis uses engineered pseudoviruses that replicate only one round, the term transduction is more appropriate than infection. Moreover, for this kind of analysis that measures viral entry, there exists a close association between pseudoviruses and live viruses [31, 65, 72].

P681 mutations within the spike do not play a role in both the neutralization potential and infectivity of SARS-CoV-2 pseudoviruses

We monitored the role of mutations within the P681 residue of the spike in affecting neutralization against a pool of our cohort and determined the viral infectivity of P681 mutated pseudoviruses in HEK293T-ACE2 cells. Our pseudo-viruses carrying spike with P681R or P681H mutations were subjected to neutralization assays against a mixture of our sera samples (**Figure 2**). Our observations show that the P681 residue has no effects on the neutralization potential of the examined sera sample. The P681R and P681H exhibited similar neutralization potential as the hCoV-19 P681 pseudovirus (**Figure 2A**). In addition, the P681H/R mutants exhibited similar infectivity levels as measured for the hCoV-19 virus (**Figure 2B**).

The fusogenic potential of hCoV-19 and its Delta or Omicron SARS-CoV-2

We next expressed spike proteins from the hCoV-19, Delta, Omicron-BA.1, and Omicron-BA.2 in Vero-E6-GFP-split cells, documenting GFP expression as a measure of cell fusion and syncytia formation between spike-expressing cells (**Figure 3A**) [56]. The hCoV-19 spike carries a Proline residue at position 681 (P681) and is part of the poly-basic motif in the spike. In the Delta spike, P681 is mutated to Arginine (R681), while in the Omicron-BA1 or Omicron-BA2, this residue is mutated to Histidine (H681). Our analysis demonstrated that expression of Delta R681 spike protein in Vero-E6 GFP split cells promoted enhanced fusion and formation of syncytia when compared to the fusion potential documented for the hCoV-19 P681 spike or to that of the Omicron lineages H681 spike (**Figure 3B**). GFP expression (area per cell) was also quantitated as a measurement for fusion potential. Image analysis and quantitation of nuclei per cell for each of the variants and cell area was calculated based on the expression of GFP and DAPI and was performed using the Scikit-image library [68] in Python 3.1 (**Figure 3C**). Our analysis confirmed the above results, showing that the Delta spike promotes efficient cell fusion relative to the hCoV-19 and Omicron spike proteins.

We also imaged cell fusion between Vero-E6 cells stably expressing either mCherry or GFP reporter proteins. Cells were mixed at equal numbers and then transfected with the indicated spike proteins from either hCoV-19, Delta, or Omicron-BA1 sub-lineage. Syncytia formation, as measured by GFP/mCherry expression overlap per nuclei, was documented using microscopy imaging (**Figure 3D**). We confirm that the hCoV-19 (P681) and Omicron-BA.1 (H681) spike proteins mediate only a modest cell fusion, as shown by their low number of syncytia. On the other hand, the Delta spike, carrying the R681 mutation, efficiently enhances fusion potential and forms syncytia.

Incorporation of spike proteins into pseudovirus particles

We next monitored levels of incorporated spike protein into pseudovirus particles. Equal amounts of pseudoviruses expressing spike from either hCoV-19, Delta, or Omicron sub-lineages were subjected to western blotting using a mono-clonal anti-spike IgG GTX632604 (GeneTex (**Figure 4**). Our analysis demonstrated that while similar levels of spike protein from the hCoV-19 and Delta were incorporated into pseudo-viral particles, the spike of Omicron BA.1 or BA.2 was incorporated less efficiently into the viral particles. p24 expression levels ensured that equal amounts of viral particles were loaded on the gel (lower panel). As the low incorporation of spike observed in the Omicron linages might be due to antibody recognition, we also confirmed our findings with a different polyclonal IgG antibody from a rabbit immunized with spike protein. Using this antibody, differences between the viral variants were more subtle (**supplementary, Figure S2**) [73]. Finally, we further monitored spike incorporation and processing in HEK293 T-producing cells. Our analysis confirmed that within producing cells, levels of spike from various SARS-CoV-2 variants and their processing were similar (**supplementary, Figure S3**).

P681 residue within the spike is important for the fusion and syncytia formation of SARS-CoV-2 pseudoviruses

As Delta and Omicron spike proteins carry a single mutation at position P681, being either P681R in Delta or P681H in Omicron (BA.1 and BA.2), we aimed to evaluate the functional significance of these mutations in promoting cell fusion and syncytia formation between target cells. Therefore, we mutated the P681 residue of the hCoV-19 spike to R681, which displayed on the spike of Delta and then expressed these two spike proteins in Vero-GFP-split cells, each expressing a GFP sub-unit. Monitoring cell fusion by microscopy for GFP expression, we documented that the P681R spike mutation of hCoV-19 led to an enhanced GFP expression, indicating that fusion and syncytia formation were restored to the levels exhibited for the Delta spike (**Figure 5A**). Conversely, switching R681 in the Delta spike to P681, which is in the hCoV-19 version, eliminated the enhanced fusion potential and syncytia formation (**Figure 5A**). We similarly mutated the spike of Omicron-BA.1 (H681) into R681 and expressed these spike proteins in Vero-GFP-split cells. We documented an enhanced fusion potential and increased syncytia formation upon mutating the Omicron-BA.1 (H681) to R681 spike (**Figure 5A).** We lastly quantitated the levels of GFP expression as a measure for fusogenic potential and syncytia formation (**Figure 5B**). We concluded that P681 in the polybasic region of the spike is critical for fusion activity and syncytia formation.

Discussion

The formation of syncytia has been documented as a hallmark of many viruses, including SARS-CoV-2 [74, 75]. The fusion of the virus with its host is mediated through the interactions of the viral spike protein that is expressed on particles with the human ACE2 receptor [76]. Although not completely understood, fusion between infected cells also takes place in the lung of infected patients, and might be linked with severe clinical symptoms and overall mortality [75, 77, 78]. Therefore, characterizing the residues within the spike that are involved in viral-cell fusion and the formation of syncytia between infected cells is critical. Along with RBD mutations within spike that have been investigated for effects on viral infectivity and neutralization sensitivity, viral variants of concern also exhibit mutations within their Furin Cleavage site (FCS) - primarily at the P681 spike position. In this study, we first used pseudoviruses to monitor the neutralization potential of sera drawn from fully vaccinated individuals four months following the administration of the third dose against the hCoV-19 SARS-CoV-2, its Delta and Omicron sub-lineages, BA.1 and BA.2, (**Figure 1**). We show that, relative to the hCoV-19, the efficiency of our sera samples to neutralize the recently emerged Omicron-BA.1 and BA.2 was substantially reduced (to about 9-12-fold). Furthermore, a decrease in the tested sera to neutralize the Delta pseudovirus was also reduced. However, this decrease in neutralization potency was lower observed with the Omicron sub-lineages and was only 2-fold relative to the hCoV-19 SARS-CoV-2.

Nevertheless, analyzed sera samples could neutralize infection of the tested pseudoviruses. We also demonstrated that Omicron-BA.1 and Omicron-BA.2 exhibited enhanced infectivity levels, which were 5-fold higher than the infectivity of the hCoV-19 pseudovirus (**Figure 1**). Overall, we conclude that the efficiency of the vaccine-elicited immune response is significantly reduced against Omicron lineages, raising concerns regarding the protection this vaccine provides against the Omicron variants. P681 residue is changed between hCoV-19 (P681), Delta (R681), and Omicron sub-linages (H681). We therefore investigated the role of this position in mediating fusion between infected cells and the formation of syncytia. Our observations show that hCoV-19 and Omicron spike proteins modestly

enhance cell fusion and syncytia formation between cells expressing the different spike proteins (**Figure 3**). In contrast, spike from the Delta SARS-CoV-2 efficiently promotes cell fusion and generates large syncytia between transduced cells (**Figure 3**). We further show that the incorporation of the spike protein into viral particles differs between the tested SARS-CoV-2 variants. Western blotting analysis shows that spike from hCoV-19, Omicron-BA.1, and Omicron-BA.2 incorporates less efficiently relative to the spike of the Delta SARS-CoV-2 variant (**Figure 4**). These observations were documented using two different spike antibodies (see also **Figure S2**). Importantly, the differences in spike incorporation levels on the surface of viral particles between the hCoV-19 SARS CoV-2 and its P681 mutants cannot explain the differences in fusogenic potential and overall viral infectivity detected for the different spike. We assume that other factors play a role in promoting syncytia formation, primarily viral infectivity that is determined by the affinity of the viral particle to its receptor as well as spike processing. Future analysis will need to be performed to better distinguish between the processes of viral infectivity and fusion and their contribution to the overall pathogenesis of the virus. Furthermore, the mutational landscape displayed within the RBD, and the furin motifs cannot dictate the overall immune response elicited by the Pfizer-BNT162b2 mRNA vaccine against any given viral variant. Thus, additional mutations within the N-terminus domain (NTD) of the spike also play a role and contribute to conformation changes of the spike that may dictate neutralization potential, fusogenicity, transmissibility, and affinity of the spike to ACE2. Indeed, residues of Omicron RBD exhibit increased electrostatic surface potential joint with a reduced affinity of the spike to the ACE2 receptor, leading to an overall lower fusogenicity potential. These parameters indicate that Omicron does not display an advantage in its infectivity levels over the Delta SARS-CoV-2. However, neutralizing epitopes that are exhibited on the spike of Omicron-BA.1 and Omicron-BA.2 protein are greatly affected, and therefore enhance the immune escape from vaccine-elicited antibodies and promote viral infection [79, 80]. In parallel, some antibodies exhibit the opposite effect and enhance viral infectivity as they promote the binding of spik to the ACE2 receptor, acquiring an open configuration of the RBD [81]. Our findings show that P681 is critical for the

fusogenic activity of the spike protein from different SARS-CoV-2 variants. Changing P681 in the hCoV-19 spike into R681, seen in Delta, restored fusogenicity and syncytia formation. Similarly, changing R681 of the Delta spike into P681 or H681 positioned within the spike of hCoV-19 or Omicron, respectively, abolishes the fusion phenotype seen in the Delta spike (**Figure 5**). The polybasic PRRAR motif is unique in the spike of SARS-CoV-2. However, its functional significance for viral infection is still not clear. Recent work has confirmed that this motif is important for viral spread, as it provides an advantage for the virus to penetrate its target cells on the cell surface by enhancing membrane fusion [56, 82, 83]. These syncytia facilitate viral replication, dissemination, and immune evasion and cause wider cytopathic effects and tissue damage. Using this entry pathway, the virus evades the IFITM2 innate response and spreads efficiently [54, 61, 84]. In viruses that are depleted of the polybasic motif, viral fusion into cells takes place in endosomes and is affected by the innate anti-viral response. In Vero E6 cells that lack TMPRSS2 and do not have an innate response, viral variants that lack FCS have an advantage due to increased spike stability and premature shedding of the S1 subunit that abolishes binding to the human receptor [85] [61]. FCS deletion also reduces infection levels due to low titers that are shed from infected cells in an animal ferrets model, leading to decreased transmission [54]. This report also showed that the TMPRSS2-mediated entry is more efficient in viruses that carry the FCS polybasic region [54]. In cell culture, the FCS sequence within the virus is lost or mutated while preserved in infectious clinical isolates. Therefore, it is possible to assume that the FCS sequence is important for viral transmission only in clinically relevant cells upon infection with the live virus [54]. In another recent work, the importance of the polybasic FCS motif was also reinforced. The P681R mutation within the spike of Kappa increased syncytia formation, contributing to enhanced infectivity also seen in Beta variants [58]. Other residues that are known to be involved in cell fusion include the D614G, K417N, and to a lesser extent E484K. However, in this work, we could not detect any effect of P681 residue on viral infectivity nor neutralization potential since the assays employed single-round pseudo-viruses and monitored only early steps of infection without extending measurements on later stages such as particle release. Moreover, we did not

conduct our analyses in clinically relevant cells, where viral infection depends on TMPRSS2-mediated fusion. Other studies have demonstrated that the Delta variant exhibits higher fusion potential compared with hCoV-19-H or Alpha P681H mutation [59, 63, 86, 87]. Omicron replicates more slowly than Delta upon expressing TMPRSS2. The use of specific inhibitors targeting the endocytic or TMPRSS2 entry pathways further led to the conclusion that while the Omicron sub-lineages mainly use the endocytic path for entry target cells, Delta SARS-CoV-2 uses both the endocytic and the TMPRSS2-dependent pathways [63]. Our study confirms these data and further defines the P681 residue within the FCS region of the spike as the key residue that dictates cell-cell fusion and syncytia formation.

Study Limitations

This work presented several limitations, mainly associated with the use of pseudoviruses. Indeed, our work uses single-round replication pseudoviruses, which are suitable for analyzing the binding of SARS-CoV-2 to its host receptor. Other reports have already demonstrated a high association between pseudoviruses and live SARS-CoV-2 viruses with regards to the attachment and entry steps of SARS CoV-2 [65, 72, 88-93]. Moreover, as we used a lentivirus system, the expression levels of the spike that are assembled on the surface of viral particles are driven according to parameters that account for lentiviruses rather than coronavirus. As such differences in the expression and assembly of the spike may take place and affect its ability to mediate fusion and syncytia formation. Finally, our findings relate only to the tested samples derived from vaccinated individuals and need to be addressed accordingly.

Author contribution statement:

Alona Kuzmina: Conceived and designed the experiments; Performed the experiments; Analyzed and interpreted the data; Contributed reagents, materials, analysis tools or data; Wrote the paper. </p>

Dina Korovin, Ido Cohen lass, Nofar Atari, Aner Ottolenghi, Pan Hu, Benyamin Rosental: Performed the experiments; Analyzed and interpreted the data; Contributed reagents, materials, analysis tools or data; Wrote the paper. </p>

Michal Mandelboim, Felipe Diaz-Griffero: Analyzed and interpreted the data; Wrote the paper. </p>

Elli Rosenberg: Conceived and designed the experiments; Wrote the paper. </p>

Ran Taube: Conceived and designed the experiments; Performed the experiments; Analyzed and interpreted the data; Wrote the paper. </p>

Data availability statement:

Data included in article/supp. material/referenced in article.

References

1. Zhou, P., et al., *A pneumonia outbreak associated with a new coronavirus of probable bat origin.* Nature, 2020. **579**(7798): p. 270-273.

2. Zhu, N., et al., *A Novel Coronavirus from Patients with Pneumonia in China, 2019.* N Engl J Med, 2020. **382**(8): p. 727-733.

3. Brouwer, P.J.M., et al., *Potent neutralizing antibodies from COVID-19 patients define multiple targets of vulnerability.* Science, 2020. **369**(6504): p. 643-650.

4. Group, A.-T.L.-C.S., et al., *A Neutralizing Monoclonal Antibody for Hospitalized Patients with Covid-19.* N Engl J Med, 2021. **384**(10): p. 905-914.

5. Rogers, T.F., et al., *Isolation of potent SARS-CoV-2 neutralizing antibodies and protection from disease in a small animal model.* Science, 2020. **369**(6506): p. 956-963.

6. Wu, Y., et al., *A noncompeting pair of human neutralizing antibodies block COVID-19 virus binding to its receptor ACE2.* Science, 2020. **368**(6496): p. 1274-1278.

7. Alsoussi, W.B., et al., *A Potently Neutralizing Antibody Protects Mice against SARS-CoV-2 Infection.* J Immunol, 2020. **205**(4): p. 915-922.

8. Gaebler, C., et al., *Evolution of antibody immunity to SARS-CoV-2.* Nature, 2021. **591**(7851): p. 639-644.

9. Walsh, E.E., et al., *Safety and Immunogenicity of Two RNA-Based Covid-19 Vaccine Candidates.* N Engl J Med, 2020. **383**(25): p. 2439-2450.

10. Anderson, E.J., et al., *Safety and Immunogenicity of SARS-CoV-2 mRNA-1273 Vaccine in Older Adults.* N Engl J Med, 2020. **383**(25): p. 2427-2438.

11. Krammer, F., *SARS-CoV-2 vaccines in development.* Nature, 2020. **586**(7830): p. 516-527.

12. Baden, L.R., et al., *Efficacy and Safety of the mRNA-1273 SARS-CoV-2 Vaccine.* N Engl J Med, 2021. **384**(5): p. 403-416.

13. Polack, F.P., et al., *Safety and Efficacy of the BNT162b2 mRNA Covid-19 Vaccine.* N Engl J Med, 2020. **383**(27): p. 2603-2615.

14. Thomas, S.J., et al., *Safety and Efficacy of the BNT162b2 mRNA Covid-19 Vaccine through 6 Months.* N Engl J Med, 2021. **385**(19): p. 1761-1773.

15. Korber, B., et al., *Tracking Changes in SARS-CoV-2 Spike: Evidence that D614G Increases Infectivity of the COVID-19 Virus.* Cell, 2020. **182**(4): p. 812-827 e19.

16. Plante, J.A., et al., *Spike mutation D614G alters SARS-CoV-2 fitness.* Nature, 2021. **592**(7852): p. 116-121.

17. Hou, Y.J., et al., *SARS-CoV-2 D614G variant exhibits efficient replication ex vivo and transmission in vivo.* Science, 2020. **370**(6523): p. 1464-1468.

18. Greaney, A.J., et al., *Complete Mapping of Mutations to the SARS-CoV-2 Spike Receptor-Binding Domain that Escape Antibody Recognition.* Cell Host Microbe, 2021. **29**(1): p. 44-57 e9.

19. Weisblum, Y., et al., *Escape from neutralizing antibodies by SARS-CoV-2 spike protein variants.* Elife, 2020. **9**.

20. Baum, A., et al., *Antibody cocktail to SARS-CoV-2 spike protein prevents rapid mutational escape seen with individual antibodies.* Science, 2020. **369**(6506): p. 1014-1018.

21. Ku, Z., et al., *Molecular determinants and mechanism for antibody cocktail preventing SARS-CoV-2 escape.* Nat Commun, 2021. **12**(1): p. 469.

22. Xie, X., et al., *Neutralization of SARS-CoV-2 spike 69/70 deletion, E484K and N501Y variants by BNT162b2 vaccine-elicited sera.* Nat Med, 2021. **27**(4): p. 620-621.

23. Giandhari, J., et al., *Early transmission of SARS-CoV-2 in South Africa: An epidemiological and phylogenetic report.* Int J Infect Dis, 2021. **103**: p. 234-241.

24. Tegally, H., et al., *Sixteen novel lineages of SARS-CoV-2 in South Africa.* Nat Med, 2021. **27**(3): p. 440-446.

25. Muik, A., et al., *Neutralization of SARS-CoV-2 lineage B.1.1.7 pseudovirus by BNT162b2 vaccine-elicited human sera.* Science, 2021. **371**(6534): p. 1152-1153.

26. Sabino, E.C., et al., *Resurgence of COVID-19 in Manaus, Brazil, despite high seroprevalence.* Lancet, 2021. **397**(10273): p. 452-455.

27. Candido, D.S., et al., *Evolution and epidemic spread of SARS-CoV-2 in Brazil.* Science, 2020. **369**(6508): p. 1255-1260.

28. Shen, X., et al., *Neutralization of SARS-CoV-2 Variants B.1.429 and B.1.351.* N Engl J Med, 2021. **384**(24): p. 2352-2354.

29. Yadav, P.D., et al., *Neutralization of variant under investigation B.1.617 with sera of BBV152 vaccinees.* Clin Infect Dis, 2021: p. 2021.04.23.441101.

30. Di Giacomo, S., et al., *Preliminary report on severe acute respiratory syndrome coronavirus 2 (SARS-CoV-2) Spike mutation T478K.* J Med Virol, 2021. **93**(9): p. 5638-5643.

31. Kuzmina, A., et al., *SARS-CoV-2 Delta variant exhibits enhanced infectivity and a minor decrease in neutralization sensitivity to convalescent or post-vaccination sera.* iScience, 2021. **24**(12): p. 103467.

32. Bar-On, Y.M., et al., *Protection of BNT162b2 Vaccine Booster against Covid-19 in Israel.* N Engl J Med, 2021. **385**(15): p. 1393-1400.

33. Iketani, S., et al., *Antibody evasion properties of SARS-CoV-2 Omicron sublineages.* Nature, 2022. **604**(7906): p. 553-556.

34. Tegally, H., et al., *Emergence of SARS-CoV-2 Omicron lineages BA.4 and BA.5 in South Africa.* Nat Med, 2022.

35. Yamasoba, D., et al., *Virological characteristics of the SARS-CoV-2 Omicron BA.2 spike.* Cell, 2022. **185**(12): p. 2103-2115 e19.

36. Yu, J., et al., *Neutralization of the SARS-CoV-2 Omicron BA.1 and BA.2 Variants.* N Engl J Med, 2022. **386**(16): p. 1579-1580.

37. Rossler, A., et al., *SARS-CoV-2 Omicron Variant Neutralization in Serum from Vaccinated and Convalescent Persons.* N Engl J Med, 2022.

38. Cele, S., et al., *Omicron extensively but incompletely escapes Pfizer BNT162b2 neutralization.* Nature, 2021.

39. Lu, L., et al., *Neutralization of SARS-CoV-2 Omicron variant by sera from BNT162b2 or Coronavac vaccine recipients.* Clin Infect Dis, 2021.

40. Cheng, S.M.S., et al., *Neutralizing antibodies against the SARS-CoV-2 Omicron variant following homologous and heterologous CoronaVac or BNT162b2 vaccination.* Nat Med, 2022.

41. Garcia-Beltran, W.F., et al., *mRNA-based COVID-19 vaccine boosters induce neutralizing immunity against SARS-CoV-2 Omicron variant.* Cell, 2022.

42. Hoffmann, M., et al., *The Omicron variant is highly resistant against antibody-mediated neutralization–implications for control of the COVID-19 pandemic.* Cell, 2021.

43. Dejnirattisai, W., et al., *SARS-CoV-2 Omicron-B.1.1.529 leads to widespread escape from neutralizing antibody responses.* Cell, 2022. **185**(3): p. 467-484 e15.

44. Pulliam, J.R.C., et al., *Increased risk of SARS-CoV-2 reinfection associated with emergence of Omicron in South Africa.* Science, 2022: p. eabn4947.

45. Cameroni, E., et al., *Broadly neutralizing antibodies overcome SARS-CoV-2 Omicron antigenic shift.* Nature, 2022. **602**(7898): p. 664-670.

46. Cao, Y., et al., *Omicron escapes the majority of existing SARS-CoV-2 neutralizing antibodies.* Nature, 2022. **602**(7898): p. 657-663.

47. Cele, S., et al., *Omicron extensively but incompletely escapes Pfizer BNT162b2 neutralization.* Nature, 2022. **602**(7898): p. 654-656.

48. Halfmann, P.J., et al., *SARS-CoV-2 Omicron virus causes attenuated disease in mice and hamsters.* Nature, 2022. **603**(7902): p. 687-692.

49. Liu, L., et al., *Striking antibody evasion manifested by the Omicron variant of SARS-CoV-2.* Nature, 2022. **602**(7898): p. 676-681.

50. Bar-On, Y.M., et al., *Protection by a Fourth Dose of BNT162b2 against Omicron in Israel.* N Engl J Med, 2022.

51. Regev-Yochay, G., et al., *Efficacy of a Fourth Dose of Covid-19 mRNA Vaccine against Omicron.* N Engl J Med, 2022. **386**(14): p. 1377-1380.

52. Magen, O., et al., *Fourth Dose of BNT162b2 mRNA Covid-19 Vaccine in a Nationwide Setting.* N Engl J Med, 2022.

53. Hoffmann, M., et al., *SARS-CoV-2 Cell Entry Depends on ACE2 and TMPRSS2 and Is Blocked by a Clinically Proven Protease Inhibitor.* Cell, 2020. **181**(2): p. 271-280 e8.

54. Peacock, T.P., et al., *The furin cleavage site in the SARS-CoV-2 spike protein is required for transmission in ferrets.* Nat Microbiol, 2021. **6**(7): p. 899-909.

55. Shi, G., et al., *Opposing activities of IFITM proteins in SARS-CoV-2 infection.* EMBO J, 2021. **40**(3): p. e106501.

56. Buchrieser, J., et al., *Syncytia formation by SARS-CoV-2-infected cells.* EMBO J, 2020. **39**(23): p. e106267.

57. Mohammad, A., J. Abubaker, and F. Al-Mulla, *Structural modelling of SARS-CoV-2 alpha variant (B.1.1.7) suggests enhanced furin binding and infectivity.* Virus Res, 2021. **303**: p. 198522.

58. Rajah, M.M., et al., *SARS-CoV-2 Alpha, Beta, and Delta variants display enhanced Spike-mediated syncytia formation.* EMBO J, 2021. **40**(24): p. e108944.

59. Saito, A., et al., *Enhanced fusogenicity and pathogenicity of SARS-CoV-2 Delta P681R mutation.* Nature, 2022. **602**(7896): p. 300-306.

60. Rajah, M.M., et al., *The Mechanism and Consequences of SARS-CoV-2 Spike-Mediated Fusion and Syncytia Formation.* J Mol Biol, 2022. **434**(6): p. 167280.

61. Winstone, H., et al., *The Polybasic Cleavage Site in SARS-CoV-2 Spike Modulates Viral Sensitivity to Type I Interferon and IFITM2.* J Virol, 2021. **95**(9).

62. Meng, B., et al., *Altered TMPRSS2 usage by SARS-CoV-2 Omicron impacts tropism and fusogenicity.* Nature, 2022.

63. Zhao, H.J., et al., *SARS-CoV-2 Omicron variant shows less efficient replication and fusion activity when compared with Delta variant in TMPRSS2-expressed cells.* Emerging Microbes & Infections, 2022. **11**(1): p. 277-283.

64. Suzuki, R., et al., *Attenuated fusogenicity and pathogenicity of SARS-CoV-2 Omicron variant.* Nature, 2022.

65. Kuzmina, A., et al., *SARS-CoV-2 spike variants exhibit differential infectivity and neutralization resistance to convalescent or post-vaccination sera.* Cell Host Microbe, 2021. **29**(4): p. 522-528 e2.

66. Krasnopolsky, S., A. Kuzmina, and R. Taube, *Genome-wide CRISPR knockout screen identifies ZNF304 as a silencer of HIV transcription that promotes viral latency.* PLoS Pathog, 2020. **16**(9): p. e1008834.

67. Schulte, B., et al., *Localization to detergent-resistant membranes and HIV-1 core entry inhibition correlate with HIV-1 restriction by SERINC5.* Virology, 2018. **515**: p. 52-65.

68. van der Walt, S., et al., *scikit-image: image processing in Python.* PeerJ, 2014. **2**: p. e453.

69. Virtanen, P., et al., *SciPy 1.0: fundamental algorithms for scientific computing in Python.* Nature Methods, 2020. **17**(3): p. 261-272.

70. Hunter, J.D., *Matplotlib: A 2D graphics environment.* Computing in Science & Engineering, 2007. **9**(3): p. 90-95.

71. Harris, C.R., et al., *Array programming with NumPy.* Nature, 2020. **585**(7825): p. 357-362.

72. Garcia-Beltran, W.F., et al., *Multiple SARS-CoV-2 variants escape neutralization by vaccine-induced humoral immunity.* Cell, 2021. **184**(9): p. 2523.

73. Makdasi, E., et al., *Neutralizing Monoclonal Anti-SARS-CoV-2 Antibodies Isolated from Immunized Rabbits Define Novel Vulnerable Spike-Protein Epitope.* Viruses, 2021. **13**(4).

74. Leroy, H., et al., *Virus-Mediated Cell-Cell Fusion.* Int J Mol Sci, 2020. **21**(24).

75. Rajah, M.M., et al., *The Mechanism and Consequences of SARS-CoV-2 Spike-Mediated Fusion and Syncytia Formation.* J Mol Biol, 2021: p. 167280.

76. Lin, L.Y., et al., *Syncytia formation during SARS-CoV-2 lung infection: a disastrous unity to eliminate lymphocytes.* Cell Death and Differentiation, 2021. **28**(6): p. 2019-2021.

77. Bussani, R., et al., *Persistence of viral RNA, pneumocyte syncytia and thrombosis are hallmarks of advanced COVID-19 pathology.* Ebiomedicine, 2020. **61**.

78. Braga, L., et al., *Drugs that inhibit TMEM16 proteins block SARS-CoV-2 spike-induced syncytia.* Nature, 2021. **594**(7861): p. 88-+.

79. Fantini, J., et al., *The puzzling mutational landscape of the SARS-2-variant Omicron.* J Med Virol, 2022. **94**(5): p. 2019-2025.

80. Fantini, J., et al., *Structural dynamics of SARS-CoV-2 variants: A health monitoring strategy for anticipating Covid-19 outbreaks.* J Infect, 2021. **83**(2): p. 197-206.

81. Liu, Y., et al., *An infectivity-enhancing site on the SARS-CoV-2 spike protein targeted by antibodies.* Cell, 2021. **184**(13): p. 3452-3466 e18.

82. Johnson, B.A., et al., *Loss of furin cleavage site attenuates SARS-CoV-2 pathogenesis.* Nature, 2021. **591**(7849): p. 293-299.

83. Lau, S.Y., et al., *Attenuated SARS-CoV-2 variants with deletions at the S1/S2 junction.* Emerg Microbes Infect, 2020. **9**(1): p. 837-842.

84. Thorne, L.G., et al., *Evolution of enhanced innate immune evasion by SARS-CoV-2.* Nature, 2021.

85. Zhang, L., et al., *SARS-CoV-2 spike-protein D614G mutation increases virion spike density and infectivity.* Nat Commun, 2020. **11**(1): p. 6013.

86. Arora, P., et al., *B.1.617.2 enters and fuses lung cells with increased efficiency and evades antibodies induced by infection and vaccination.* Cell Rep, 2021. **37**(2): p. 109825.

87. Zhang, J., et al., *Membrane fusion and immune evasion by the spike protein of SARS-CoV-2 Delta variant.* Science, 2021. **374**(6573): p. 1353-1360.

88. Wang, P., et al., *Increased resistance of SARS-CoV-2 variant P.1 to antibody neutralization.* Cell Host Microbe, 2021. **29**(5): p. 747-751 e4.

89. Wang, W., et al., *Detection of SARS-CoV-2 in Different Types of Clinical Specimens.* JAMA, 2020. **323**(18): p. 1843-1844.

90. Ju, B., et al., *Human neutralizing antibodies elicited by SARS-CoV-2 infection.* Nature, 2020. **584**(7819): p. 115-119.

631 91. Pinto, D., et al., *Cross-neutralization of SARS-CoV-2 by a human monoclonal SARS-*
632 *CoV antibody.* Nature, 2020. **583**(7815): p. 290-295.

633 92. Yan, R., et al., *Structural basis for the recognition of SARS-CoV-2 by full-length*
634 *human ACE2.* Science, 2020. **367**(6485): p. 1444-1448.

635 93. Crawford, K.H.D., et al., *Protocol and Reagents for Pseudotyping Lentiviral Particles*
636 *with SARS-CoV-2 Spike Protein for Neutralization Assays.* Viruses, 2020. **12**(5).
637

638

Main Figures and legends

Figure 1: The neutralization potential of post-vaccinated sera against SARS-CoV-2 pseudoviruses and its variants of concern

A. Relative neutralization sensitivity of Delta, Omicron-BA.1, and Omicron-BA.2 sub-lineages – Measurements of neutralization were performed with sera samples of individuals vaccinated with the third dose of the Pfizer-BNT162b2 vaccine and drawn four months post-administration. For neutralization measurements, sera samples (n=35) were incubated with the indicated pseudoviruses, and then HEK293T-ACE2 target cells were tranduced. 72 hours later, transduction levels were analyzed by reading luciferase levels. Neutralizing potential was calculated following transduction of pseudoviruses in the presence of increased serial dilutions of the sera sample, and was determined relative to transduced cells where no sera were supplemented. NT_{50} neutralization is the inverse dilution that achieves 50% neutralization levels. The results are the average of two experiments. For each experiment, the indicated sera samples were diluted (for each sera, 5-6 dilutions were made) and analyzed against the pseudovirus. For each dilution point, three independent dilutions were performed and analyzed. Black bars represent the geometric mean of NT_{50} values, indicated at the top. Statistical significance was determined using a two-tailed t-test ***$p<0.001$. The fold of the average NT_{50} decrease is calculated relative to the HCoV-19 strain.

B. Relative infectivity levels of hCoV-19, Delta and Omicron- BA.1 BA.2 sub-lineages HEK293T-ACE2 target cells were transduced with pseudoviruses carrying spike from hCoV-19 SARS-CoV-2, its Delta or Omicron-BA.1 and Omicron-BA.2 spike proteins. Viral load was normalized based on measuring p24 levels. 48 hours post-transduction, cells were harvested and luciferase readouts were measured. Three independent infection experiments were performed. Bar graphs show mean values ± SD error bars of three independent experiments.

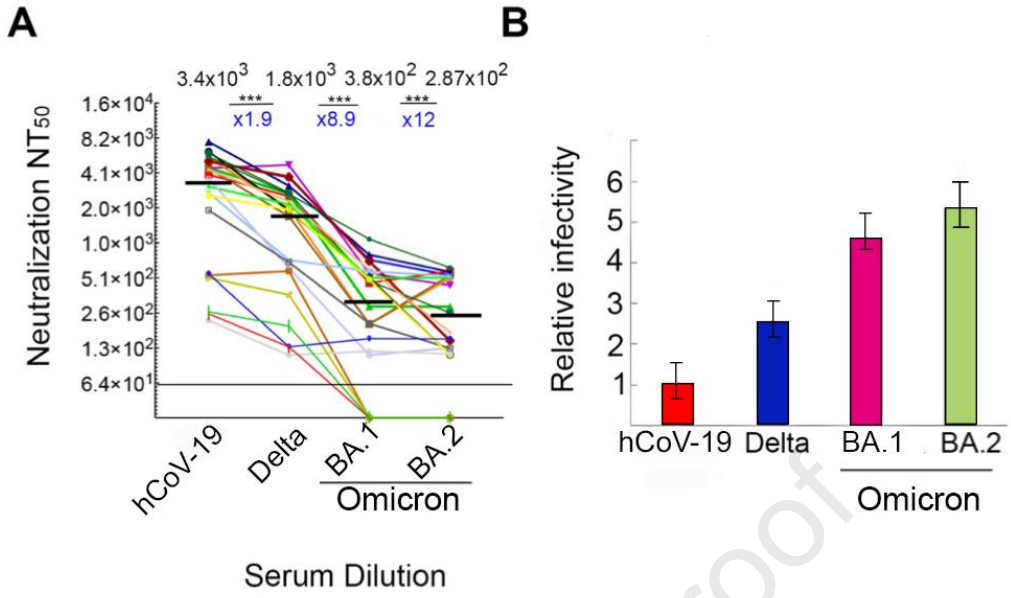

Figure 1

669 **Figure 2: P681 residue of spike protein has no role in neutralization potential and infectivity of**
670 **SARS-CoV-2 pseudoviruses**

671 **A. Neutralization sensitivity of SARS-CoV-2 pseudoviruses with P681 spike mutations** -
672 neutralization analyses were performed in the presence of a pool of sera samples (n=35) drawn from
673 individuals vaccinated with the third dose of the Pfizer-BNT162b2 vaccine and drawn four months
674 post-administration. For neutralization measurements, sera samples were incubated with the indicated
675 pseudoviruses for one hour, followed by the transduction of HEK293T-ACE2 target cells. 72 hours
676 post-transduction, cells were harvested, and their transduction was monitored by measuring luciferase
677 readings. Neutralizing potency was calculated in the presence of increased serial dilutions of the
678 mixed sera samples and are presented relative to cells that were transduced with no sera added.
679 Neutralization, NT_{50} is defined as the inverse dilution that achieved 50% neutralization. Presented
680 results are an average of two independent biological assays. For each experiment, the indicated sera
681 samples were diluted (for each serum, 5-6 dilutions were made) and analyzed against the pseudovirus.
682 For each dilution point, three independent dilutions were performed and analyzed. Black bars
683 represent the geometric mean of NT_{50} values, indicated at the top. Statistical significance was
684 determined using a two-tailed t-test ***$p<0.001$. The fold of the average NT_{50} is calculated relative
685 to the hCoV-19 strain.

686 **B. Relative infectivity levels of SARS-CoV-2 pseudoviruses carrying P681 mutations**
687 Pseudoviruses expressing the hCoV-19 SARS-CoV-2 spike or its P681R or P681H spike proteins
688 were used to transduce HEK293T-ACE2 target cells. Equal viral loads were normalized based on p24
689 protein levels. 48 hours post-transduction, cells were harvested, and their luciferase readouts were
690 monitored. Three independent infection experiments were performed. Bar graphs show mean values
691 ± SD error bars of three independent experiments.
692

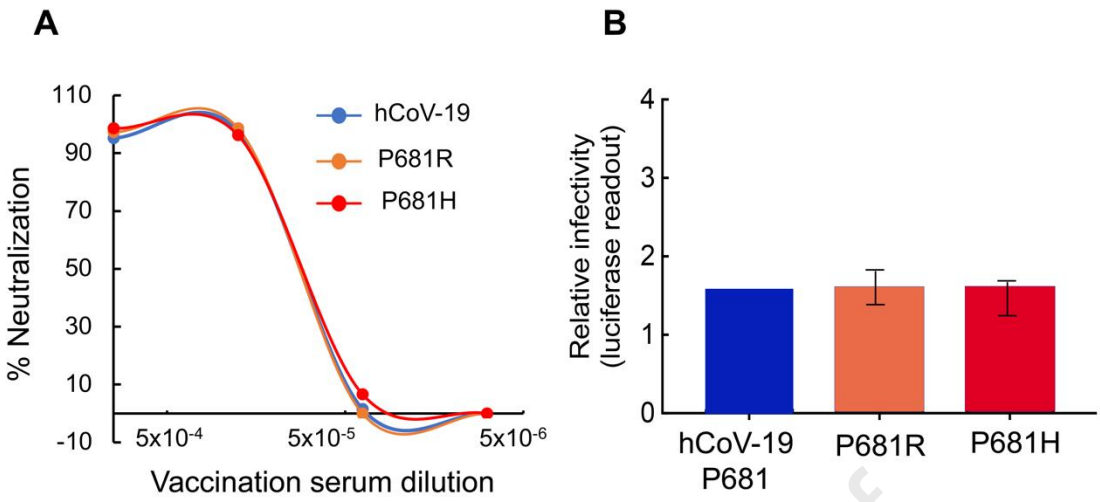

693
694
695

Figure 2

Figure 3: Delta spike promotes enhanced fusogenic activity and syncytia formation relative to the spike of hCoV-19 and Omicron BA.1 or BA.2 sub-lineages of SARS-CoV2

A. Vero E6-GFP 10 and 11 represent cells expressing each GFP subunit. GFP is expressed only upon cell fusion and is solely dependent on the spike of SARS-CoV-2 [58].

B. Vero-E6-GFP split cells were transfected with the indicated spike proteins from hCoV-19, Delta, Omicron- BA.1, and Omicron-BA.2. 48 hours post-transfection, cells were imaged for their GFP expression as an indicator for cell fusion.

C. Quantification of fusion potentials for hCoV-19, Delta, Omicron-BA.1, and Omicron-BA.2 spike proteins. Quantification was performed by imaging GFP and DAPI expression and calculating the number of nuclei per cell and cell area as a measurement of fusion. Image analysis and quantitation were calculated based on the expression of GFP area and DAPI and were performed using the Scikit-image library in Python 3.1.[68]

D. Visualization of fusion and syncytia formation – Vero-E6 cells stably expression either mCherry or GFP were transfected with the indicated spike. 48h post-transfection cells were imaged for syncytia formation that measured the merged expression of mCherry and GFP using a Zeiss microscope.

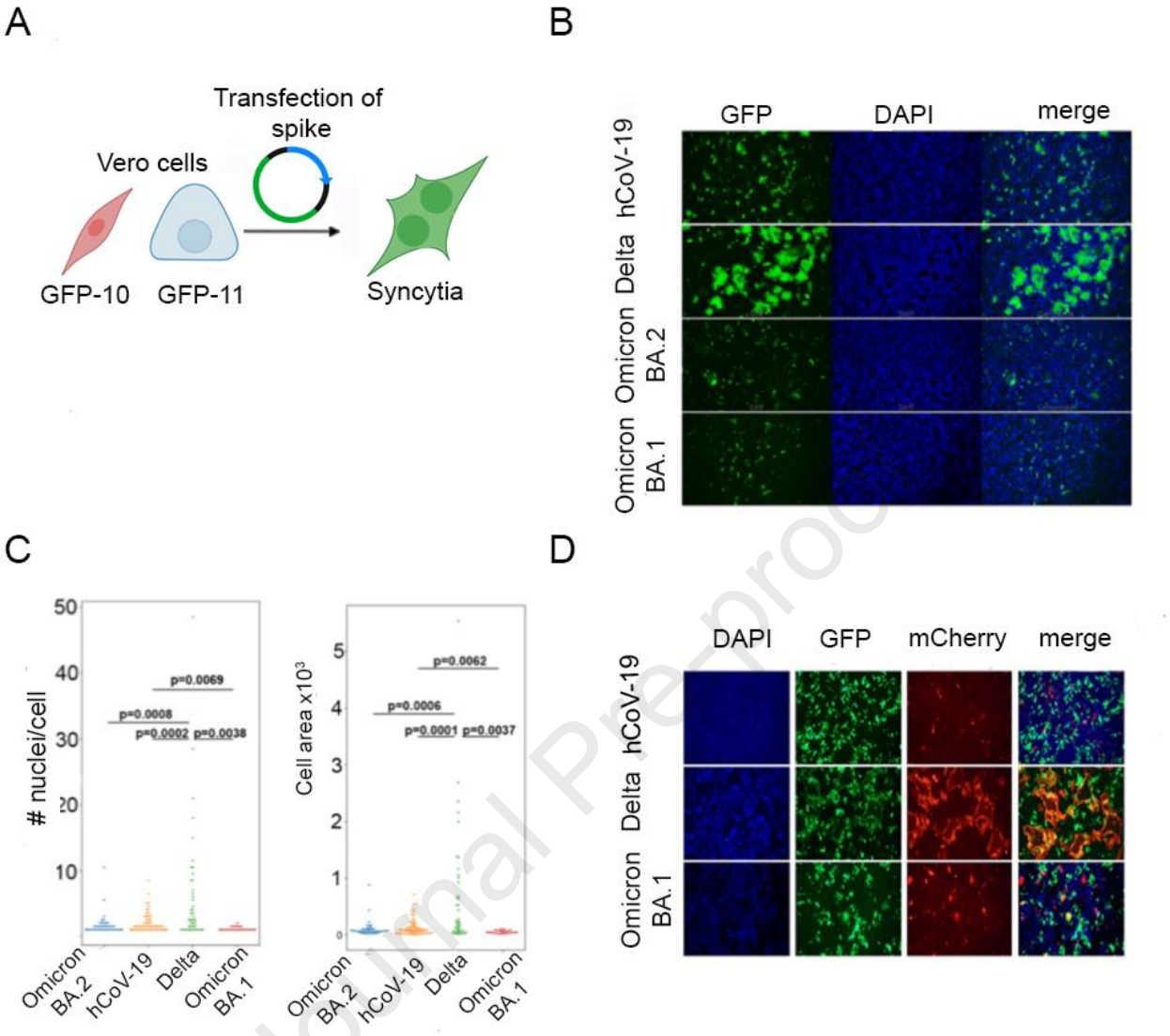
A
Transfection of spike
Vero cells
GFP-10
GFP-11
Syncytia
B
GFP
DAPI
merge
hCoV-19
Delta
Omicron BA.2
Omicron BA.1
C
# nuclei/cell
p=0.0069
p=0.0008
p=0.0002
p=0.0038
Cell area x10³
p=0.0062
p=0.0006
p=0.0001
p=0.0037
Omicron BA.2
hCoV-19
Delta
Omicron BA.1
D
DAPI
GFP
mCherry
merge
hCoV-19
Delta
Omicron BA.1

Figure 3

Figure 4: Spike from Omicron-BA.1 and Omicron-BA.2 incorporate less efficiency into viral particles relative to hCoV-19 and Delta pseudoviruses

A. Concentrated pseudotyped viral particles with the indicated SARS-CoV-2 spike were lysed and equally loaded on an SDS-PAGE gel, followed by western blotting using an α-spike GTX632604 (Genetex) and anti-p24 (NIH repository) antibodies. The lower panel represents a western blot with p24 for an equal load of viruses. Arrowheads indicate spike proteins.

B. Intensity analysis of spike bands using image J, normalized to p24 levels and shown relative to the hCoV-19 spike levels set to 100%. Two independent experiments were performed. Bar graphs show mean values ± SD error bars of two independent experiments. Statistical significance of our study was determined by a two-tailed Student's t-test - P≤0.001. Error bars show standard deviation.

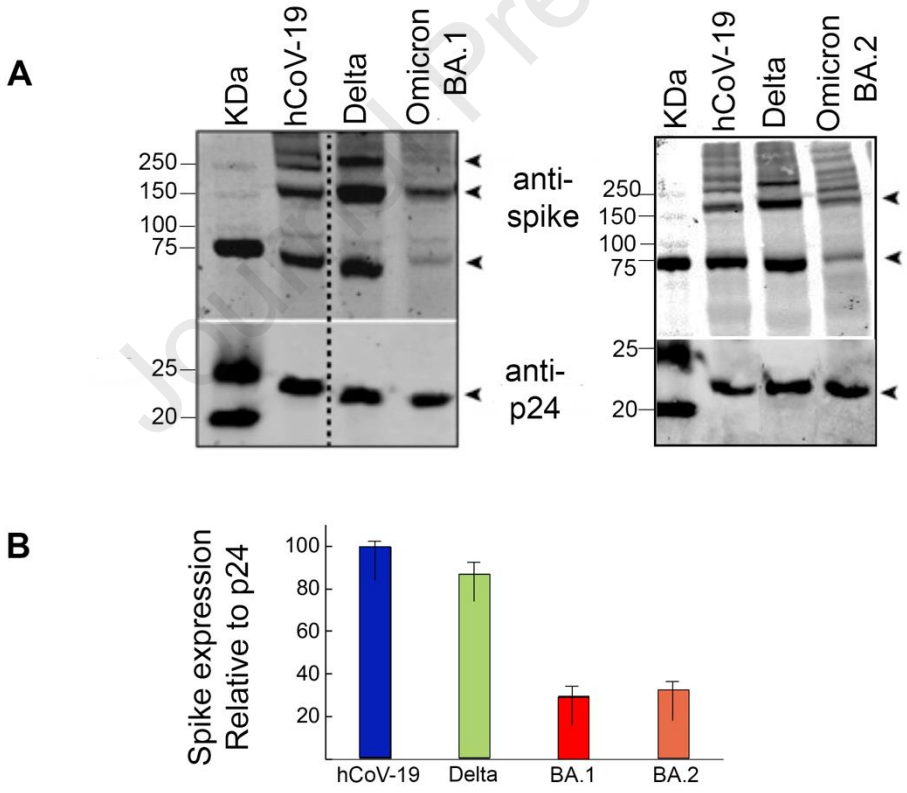

Figure 4

Figure 5: P681 residue of spike dictates cell fusion and syncytia formation of SARS-CoV-2

A. Equal cell numbers of Vero-E6 cells expressing either GFP1-10 or GFP 11 (Vero GFP-split) were seeded together and then transfected with the indicated spike from either hCoV-19, Delta, or Omicron. 72 hours post-transfection, cells were monitored for their GFP expression by microscopy to measure cell-fusion potential. The top images represent cell fusion upon expressing the hCoV-19 (P681), Delta (R681), and Omicron-BA.1 (H681). The bottom images represent cell fusion upon expressing HCoV-19-P681R, Delta- R691P, and Omicron H681R.

B. Quantitation of fusogenicity using image J (GFP area/number of nuclei).

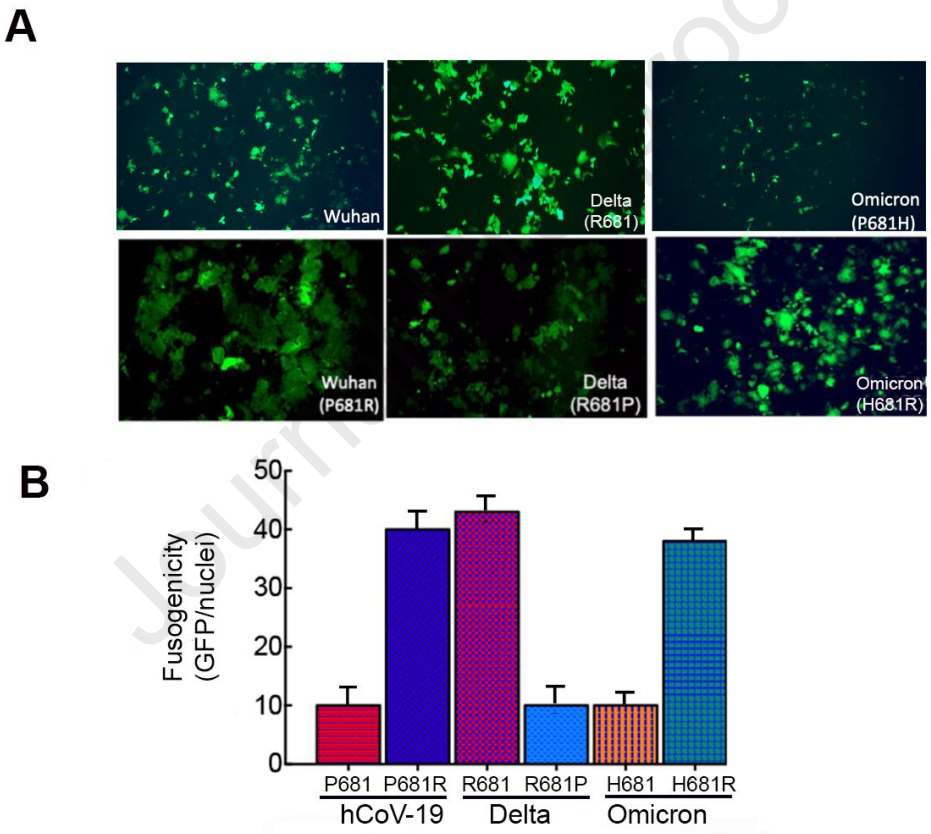

Figure 5

765 **Supplementary**

766 **Figure S1: TMPRSS2 has no effects on viral infectivity of pseudoviruses that infect HEK-**
767 **293T-ACE2-TMPRSS2**

768 **A.** Pseudoviruses bearing the indicated SARS-CoV-2 spike P681 mutations were used to
769 transduce HEK-ACE2 cells and HEK cells that express HA-TMPRSS2. The human protease was
770 transfected into cells 48hr earlier and its expression was verified in infected cells by FACS (panel A).
771 Equal viral loads were normalized based on p24 protein levels. 48hr post transduction, cells were
772 harvested and their luciferase readouts were monitored. Bar graphs show mean values ± SD error
773 bars of three independent experiments. Measured statistical significance was calculated between
774 experiments by a two-tailed Student's t test ***P≤0.001.

775 **B.** Control HEK-293 non-transfected cells and cells that stably express TMPRSS2-HA were
776 dissociated by EDTA treatment, and washed with PBS-0.01% Tritin washing buffer. Cells were then
777 incubated with 0.04% triton for 10 min on ice, washed and blocked with 4% FCS in PBS. Cells were
778 then incubated with anti-HA IgG (5 µg/ml, Abcam ab9110) for 45 min on ice. After x3 washes with
779 washing buffer, the cells were incubated with Rhodamine-Red labeled goat anti-
780 Rabbit IgG antibody (1:200; Jackson 111-296-003), washed x3 times with washing buffer and
781 analyzed by FACS.

782

783

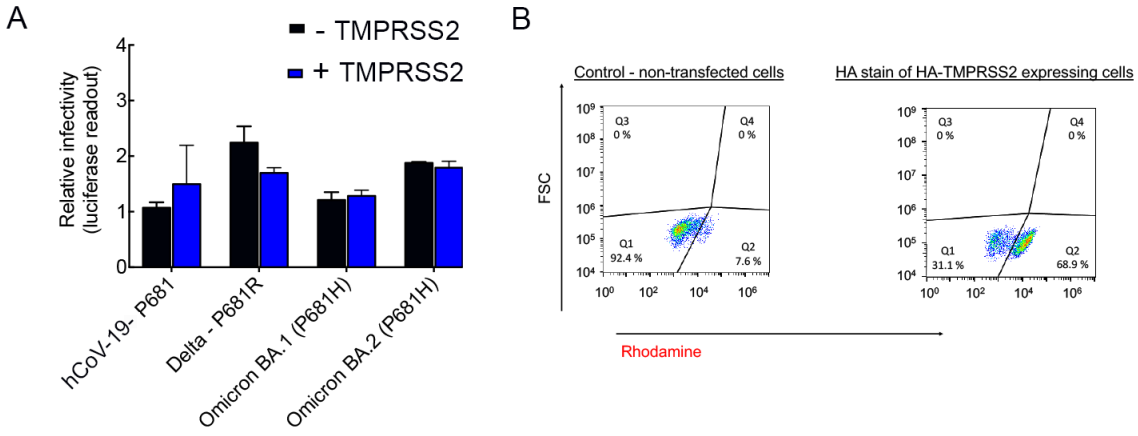

784

Figure S2: Omicron-BA.1 and Omicron-BA.2 pseudoviruses display lower levels of spike relative to hHCoVCoV-19 and Delta pseudoviruses

A. Concentrated HIV particles pseudotyped with the indicated SARS-CoV-2 spike were lysed and equally loaded on SDS-PAGE, followed by western blot analysis using a polyclonal IgG antibody from a rabbit immunized with spike protein [73], and anti-p24 (NIH repository) antibodies. The lower panel represents a western blot with p24 for an equal load of viruses.

B. Intensity analysis of spike bands using image J, normalized to p24 levels and shown relative to the hCoV-19 spike levels set to 100%. Two independent experiments were performed. Bar graphs show mean values ± SD error bars of two independent experiments. Statistical significance of our study was determined by a two-tailed Student's t-test - P≤0.001. Error bars show standard deviation.

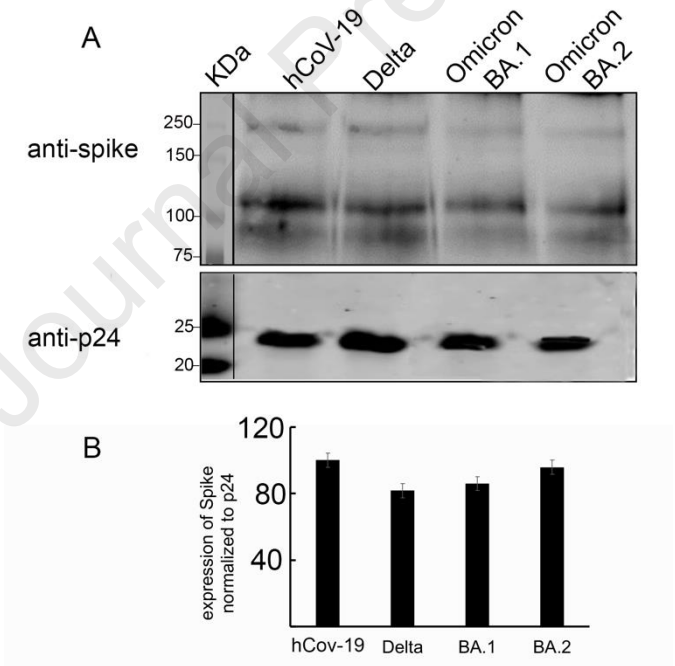

Figure S3: Expression and processing of spike in producer cells expressing spike SARS CoV-2

A. Cell lysate of HEK-293T cells expressing the indicated spike protein was subjected to SAS-PAGE and western blot using anti-spike IgG. Spike expression plasmids were transfected into producer cells using lipofectamine. 48hr post transfection cells were harvested lysed and equally loaded on SDS-PAGE, followed by western blot analysis using anti-spike GTX632604 (Gene tex) and anti-p24 (NIH repository) IgG. The lower panel represents a western blot with p24 for an equal load of viruses.

B. Intensity analysis of spike bands using image J, normalized to p24 levels and shown relative to the hCoV-19 spike levels set to 100%. Two independent experiments were performed. Bar graphs show mean values ± SD error bars of two independent experiments. Statistical significance of our study was determined by a two-tailed Student's t-test - P≤0.001. Error bars show standard deviation.